ELSEVIER

NeuroImage

www.elsevier.com/locate/ynimg
NeuroImage 30 (2006) 172-183

Cortical plasticity following surgical extension of lower limbs

F. Di Russo,[a,b,*] G. Committeri,[a,d] S. Pitzalis,[a,c] G. Spitoni,[a,c] L. Piccardi,[a,c] G. Galati,[a,d] M. Catagni,[e] D. Nico,[a,c] C. Guariglia,[a,c] and L. Pizzamiglio[a,c]

[a]*Santa Lucia Foundation IRCCS, Rome, Italy*
[b]*Department of Education in Sport and Human Movement, University for Human Movement "IUSM", Rome, Italy*
[c]*Department of Psychology, University of Rome "La Sapienza", Rome, Italy*
[d]*Department of Clinical Sciences and Bioimaging, University of Chieti "G. d'Annunzio", Chieti, Italy*
[e]*Department of Orthopaedic and Ilizarov Unit, Lecco General Hospital, Lecco, Italy*

Received 10 June 2005; revised 6 September 2005; accepted 7 September 2005

Human cortical plasticity has been studied after peripheral sensory alterations due to amputations or grafts, while sudden 'quasi-physiological' changes in the dimension of body parts have not been investigated yet. We examined the cortical reorganization in achondroplastic dwarfs submitted to progressive elongation (PE) of lower limbs through the Ilizarov technique. This paradigm is ideal for studying cortical plasticity because it avoids the perturbation connected with deafferentation and reafferentation. Somatosensory evoked-potentials (SEP) and fMRI studies were performed before and after PE during foot and knee stimulation, above and below the surgical fracture. A body schema test was also performed. Following PE, cortical modifications were observed in the primary somatosensory cortex for foot stimulation and in higher order somatosensory cortices for foot and knee. The former modifications tended to decrease 6 months after the elongation ending, whereas the latter tended to persist. Results are interpreted in terms of cortical adaptation mediated by temporary disorganization.

Keywords: Cerebral plasticity; Achondroplasia; SEP; MRI; fMRI; Source analysis; Co-registration; Brain mapping; Ilizarov

Introduction

Cortical plasticity in the adult brain has been primarily documented in animals and humans following peripheral nerve suppression (transient or permanent), peripheral sensory stimulation and limb amputation (i.e., Knecht et al., 1991; Ramachandran et al., 1992; Flor et al., 1995; Buonomano and Merzenich, 1998; Dettmers et al., 1999, 2001; Wall and Wang, 2002; Diamond et al., 2003). Few studies in humans have described the development of plastic changes over time. Two studies have documented the motor and sensory consequences of arm amputation and grafts. Giraux et al. (2001) showed that after amputation, but before grafting, hand representations were restricted to the more lateral portion of normal cortical representations (towards the face), while 6 months after the graft, there was an early expansion followed by a shift toward the location normally activated during hand movements. The reversibility of cortical representation was studied in the same patient (CD) also in the sensory functional reorganization domain (Farné et al., 2003). The authors showed that simultaneous tactile stimulation of the face extinguished hand tactile stimulation before the graft (in accordance with the post-amputation altered representation) and 6 months after, but no more than 11 months post-operatively. Both results suggest that the reafferentation of motor and sensory cortices due to the transplant produced the progressive return to the standard cortical representation, which existed prior to the amputation.

In the present research, we studied cortical reorganization in patients who underwent a different surgical procedure to increase the length of their lower limbs. Ilizarov and Deviatov (1971) and Cattaneo et al. (1988a) introduced this procedure many years ago. The Ilizarov technique (Fig. 1) for distraction osteogenesis is accepted as a worthwhile option in selected cases of massive segmental bone loss. In this technique, the cortex of the bone is partially cut, leaving the medulla intact; an external steel cage, fixed on the bones (fixation), progressively distracts the two bone segments by about 1 mm a day. This progressive elongation (PE) prevents the formation of a callus and, thus, the physiological reconnection of the two parts of the bones. When the desired length is reached, the callus is allowed to solidify; the steel cage is removed only when the two parts of the bone consolidate their cortical structure.

The Ilizarov technique is used to lengthen the limbs of achondroplastic (ACH) (Cattaneo et al., 1988b) or traumatic patients (e.g., Birch and Samchukov, 2004) who have suffered

* Corresponding author. Department of Education in Sport and Human Movement, University for Human Movement "IUSM", Piazza Lauro De Bosis, 15, 00194 Rome, Italy. Fax: +39 06 36733387.
E-mail address: fdirusso@iusm.it (F. Di Russo).
URL: http://www.webalice.it/fdirusso/FDR (F. Di Russo).
Available online on ScienceDirect (www.sciencedirect.com).

1053-8119/$ - see front matter © 2005 Elsevier Inc. All rights reserved.
doi:10.1016/j.neuroimage.2005.09.051

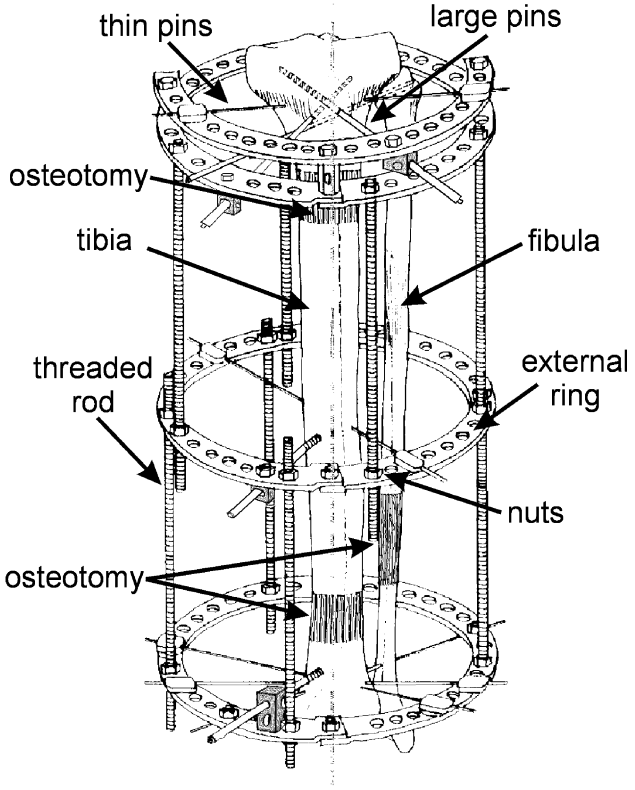

Fig. 1. Schematic representation of the Ilizarov bone-lengthening device, which connects to the patient limb by a series of pins that have been drilled through the bones (tibia and fibula). The *osteotomy* is where the bone is surgically cut to begin the lengthening process. The nuts have to be turned 4–6 times per day.

from a considerable shortening of a limb. This artificially induced PE of approximately 10–15 cm normally occurs in less than 1 year and probably requires a rearrangement of both motor and somatosensory cortical maps of the expanded limbs, as well as psychophysical changes in body perception. This surgical procedure constitutes an ideal model for studying brain plasticity following the sudden growth of a body segment in a quasi-physiological way and avoids the complex perturbation connected with the reafferentation of the transplants.

In the present experiment, two young ACH patients who underwent PE of both legs were studied at various stages using different techniques including somatosensory evoked-potentials (SEPs), structural and functional magnetic resonance imaging (MRI) and behavioral testing to describe any cortical, peripheral and cognitive changes in the patients' body representation. Multichannel SEPs were evoked by stimulation below (foot) and above (knee) the surgical fracture of both lower limbs, before surgery (pre-test) and 15 days after PE ended (post-test) to illustrate the spatio-temporal evolution of the cortical sensorial afferences. One patient also underwent a third evaluation 6 months later (follow-up). In this patient, fMRI signal in response to right foot and knee stimulation was recorded at the three temporal stages. Moreover, the subjects' body representation was assessed behaviorally using a body schema (Daurat-Hmeljiak et al., 1978) test at the same time points (pre, post and follow-up) and during the immobilization phase (i.e., with the fixation cage on). To improve the spatial resolution of SEPs and the temporal resolution of fMRI, we combined SEP recording, MRI and fMRI mapping with cortical surface reconstruction of each individual brain to account for the morphometric abnormalities observed in ACH patients (Mueller, 1980; Di Mario et al., 1995; Thompson et al., 1999). Besides obvious peripheral changes, we expected to find significant perceptual and cerebral rearrangements at the end of the lengthening procedure, documenting the evolution of these changes over time.

Materials and methods

Participants

Two young achondroplastic patients (a girl of 14 and a boy or 15 years of age) and two sex- and age-matched volunteers participated in the main SEP experiments. Table 1 shows the main features of the participants, who were all right-handed and had normal or corrected-to-normal visual acuity. Both patients received anatomical MRI scans, but only DM participated in both the fMRI and the behavioral study. The ACH patients had abnormal body proportions; arms and legs were very short, while the torso was nearly the normal size. Their cognitive skills fall within the normal range (DM: WISC-R verbal IQ = 108, Performance IQ = 87, Total IQ = 98; RZ: WISC-R verbal IQ = 94, Performance IQ = 88, Total IQ = 90). After the PE, their height increased 15 cm (DM) and 13 cm (RZ). As expected, instead, the physiological height increase of the two young normal volunteers in 6 months was much smaller (about 4 cm). Written informed consent, approved by the local ethical committee, was obtained from all participants, and parents after the procedures had been fully explained to them.

SEP experiment

Stimuli and procedure

Subjects lay comfortably on a bed in a sound-attenuated and electrically shielded room. SEPs were recorded in response to non-painful electric stimulation of left and right tibial nerves at level of the foot and ankle by skin electrodes (areas below and above the surgical fracture). Each run, 2 min in duration, was followed by 2 min of rest. A total of 2000 trials were averaged for each condition. Stimulus intensity was adjusted at slightly more than 1.5 times the motor threshold to obtain a similar stimulation level for stimulated locations, sessions and subjects. The stimulation rate was 3 Hz and the length of the electric impulse 50 μs. Subjects were trained to maintain stable fixation on a comfortable point to avoid eye movements.

Table 1
Main features of the participants

	Age	Sex	Subject height (cm)			Height increase (cm)
			Pre-test	Post-test	Follow-up	
Patients						
RZ	14	F	139	152		13
DM	15	M	130	145	145	15
Controls						
SB	15	F	156	159		3
PFG	15	M	161	166		5

Note. M = male; F = female. Controls and patient RZ were tested in the SEP experiment only.

Patients were tested twice: 15 days before surgery (pre-test), and 6 months after surgery, i.e., 15 days after removal of the Ilizarov fixation (post-test). Patient DM also received a third evaluation, 6 months after the post-test (follow-up). To check the effect of natural growth, controls were tested twice with an interval of 6 months between the first and the second evaluation.

Electrophysiological recording and data analysis

The EEG was recorded from 64 electrodes using the international 10–10 system montage (Di Russo et al., 2002). All scalp channels were referenced to the mastoid ipsilateral to the side of stimulation (M1 or M2); a non-cephalic ground was placed on the stimulated thigh. Horizontal eye movements were monitored with a bipolar recording from electrodes at the left and right outer canthi. Blinks and vertical eye movements were recorded with an electrode below the left eye, which was referenced to Fp1. The EEG from each electrode site was digitized at 5000 Hz with an amplifier bandpass of 0.01 to 1000 Hz and was stored for off-line averaging. Electrical activity was recorded using the BrainProducts^{Tm} 64-channels system. Computerized artifact rejection was performed prior to signal averaging in order to discard epochs in which deviations in eye position, blinks, or amplifier blocking occurred. Muscle tension was the most frequent cause for rejection. SEPs were averaged separately for each stimulation in epochs that began 20 ms prior to the electric pulse and lasted for 220 ms. To further reduce high- and low-frequency noise, the averaged SEPs were digitally band-pass filtered from 10 to 200 Hz (zero phase Butterworth filter, 6 dB/octave slope). The amplitudes of the different SEP components were measured as peak values within specified windows with respect to the 20 ms pre-stimulus baseline. Middle latency SEP components P35 for knee stimulation and P40 for foot stimulation were studied, since they represent the earliest cortical responses to tibial nerve stimulation from Broadman area 3b of SI (e.g., Valeriani et al., 2000).

Modeling of SEP sources

Topographical maps of scalp voltage over time were obtained for the SEPs to each stimulus. Estimation of the dipolar sources of SEP components was carried out using Brain Electrical Source Analysis (BESA 2000 version 5.1, MEGIS, Germany). The BESA algorithm estimates the location and the orientation of multiple equivalent dipolar sources by calculating the scalp distribution that would be obtained for a given dipole model (forward solution) and comparing it to the actual SEP distribution. Interactive changes in the location and orientation of the dipole sources lead to minimization of the residual variance (RV) between the model and the observed spatio-temporal SEP distribution. This analysis used a realistic approximation of the head by using a spatial digitizer recording to obtain the subjects' radius. A computer algorithm was used to relate the subject's head on the standardized finite element model of BESA 2000 to improve spatial resolution (more details on Di Russo et al., 2005). Furthermore, the individual MRI of the two patients was used to display dipole position. As a modeling strategy, in all subjects, an unseeded model was fitted over specific latency ranges (given below) in location and orientation to account for the first cortical SEP component. A single dipole was fitted in the interval between 35–45 ms post-stimulus for the P40 component and in the 30–40 ms interval for the P35 component. For patient DM, and for the right limb only, the centers of gravity (COGs) of the fMRI activation in SI (see fMRI method below) were used to constrain the locations of the dipoles in a new seeded model in order to improve the spatial resolution of the dipoles. In this seeded model, dipole orientations were fitted over the same time intervals used in the unseeded model.

Neuroimaging session

All MR examinations were conducted at the Santa Lucia Foundation (Rome, Italy) on a 1.5 T Vision MR scanner (Siemens Medical Systems) equipped for echo-planar imaging.

Anatomical image processing

Both patients underwent an anatomical acquisition session. Two high-resolution T1-weighted images of the whole brain were acquired using a head coil and a 3D Magnetization Prepared Rapid Gradient Echo (MPRAGE) sequence (TR = 11.4 ms, TE = 4.4 ms, 10° flip angle, 1 × 1 × 1 mm resolution, 220 coronal slices), tuned to optimize the contrast between gray and white brain matter. The cortical surfaces of the two patients were reconstructed and inflated from the anatomical images using the FreeSurfer software as detailed elsewhere (Dale et al., 1999; Fischl et al., 1999). The cortical surface reconstructions (pial surface) were used in the SEP experiment to show the cortical position of the dipoles on the patients' brains. In the case of patient DM, using MRIcro software (Rorden and Brett, 2000), we manually drew a ROI of the contralateral SI, which was subsequently used to mask the functional activation. SI-ROI included the cortical tissue from the posterior wall of the central sulcus to the posterior border of the post-central gyrus, considered the hallmarks of SI (e.g., Talairach and Tournoux, 1988; Duvernoy, 1991).

Achondroplasia implies several abnormal physical characteristics including (crucially for the present study) a typically enlarged head and dilated cerebral ventricles (Mazziotta et al., 1995). Neuroanatomic abnormalities were found also in the medulla and corpus callosum (Di Mario et al., 1995) and in the frontal lobes (Thompson et al., 1999). Thus, the use of a carefully reconstructed cortical surface of the patients' brains (instead of an anatomical template) is a necessary methodological refinement.

Apparatus and fMRI procedures

Patient DM underwent three fMRI acquisition sessions at the same time intervals of the SEP experiment. In each session, we acquired two runs of fMR images during right foot tactile stimulation and two runs during right knee tactile stimulation. We used a two-condition block sequence paradigm (ON vs. OFF), where the tactile stimulation and the baseline (period without stimulation) were presented in direct alternation, in 32-s epochs, using 8 epochs per scan. DM was instructed to keep his eyes closed, to relax and to avoid even minimal movements. Non-painful tactile stimuli were manually delivered by an experimenter standing in the scanner room at the subject's side. A plastic brush with pointed bristles was scrubbed on the patient's foot (big toe and toes) or knee in lateral–medial direction, at a frequency of ~1 Hz. Prior to entering the scanner, DM was asked to subjectively quantify the perceived magnitude of the stimulus intensities so as to use a non-painful but still intense stimulation and to roughly match the stimulus perceived magnitude across sessions. Echo-planar functional images based on BOLD contrast were acquired in runs of 128 consecutive volumes (TR = 2 s, TE = 42 ms, 90° flip angle, bandwidth = 926 Hz/pixel, 3 × 3 mm in-plane resolution, 16

contiguous 4-mm thick slices), using a small flex quadrature surface RF coil placed over parietal areas and the region of the central sulcus.

Functional image processing

Functional images were pre-processed and analyzed using SPM99 (Wellcome Department of Cognitive Neurology, London, UK). They were corrected for head movement and manually co-registered to the subject's anatomical image. Images were not smoothed, so as to avoid losing spatial resolution. Images were analyzed using a general linear model, where experimental blocks were modeled as box-car functions, convolved with a canonical hemodynamic response function. Statistical parametric maps of the T statistics were computed for foot and knee activation in each of the three acquisition sessions (i.e., six conditions), with a threshold of $P < 10^{-4}$ or higher (uncorrected), while also imposing an

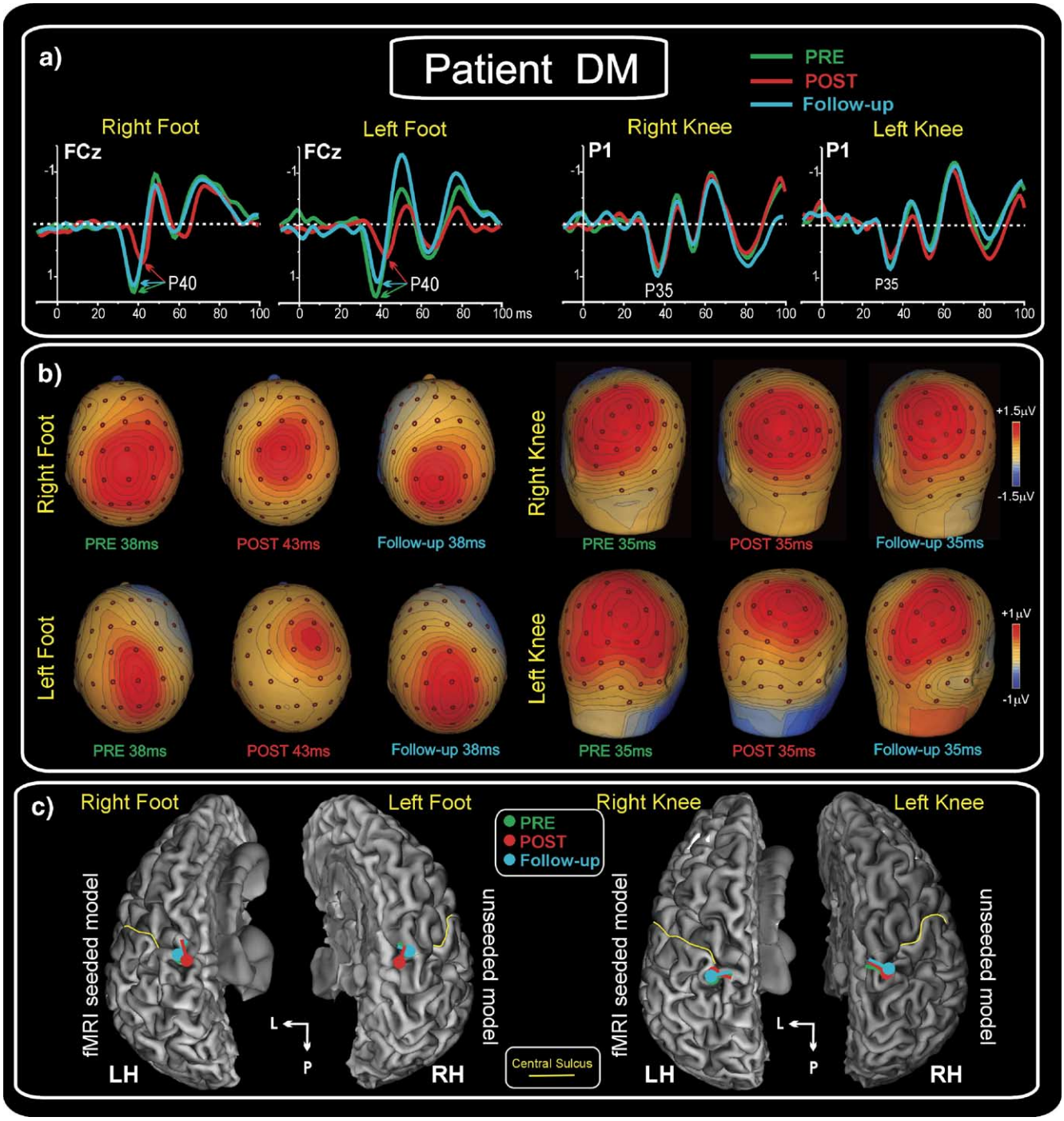

Fig. 2. SEP data of patient DM in the pre-surgery, post-surgery and follow-up sessions: (a) SEP waveforms showing the first P40 and P35 cortical component for foot and knee stimulation, respectively. (b) Scalp topography of P40 and P35 components. (c) Source model of studied components projected on the patient's anatomy. Dipoles for right stimuli are seeded on the fMRI activations. Dipoles for left stimuli are based on SEP only. Logos indicates two main orthogonal directions (anterior–posterior and medial–lateral).

activation extent threshold of at least two adjacent voxels. For the significantly activated voxels in the SI-ROI, we computed the center of gravity (COG) as the average of the coordinates of each voxel, weighted by the voxel Z score. For activation outside SI, instead, we defined three functional ROIs (contralateral superior parietal lobule or SPL, ipsilateral SPL and contralateral inferior parietal lobule or IPL) including the clusters which were significantly activated by at least one of the six conditions. For each ROI, a representative time course was computed in terms of the first eigenvariate of the raw fMRI signal in all voxels of the ROI. A second general linear model was fitted to the ROI time course and used to test for the presence of significant differences between the pre-test, post-test and follow-up sessions for both foot and knee at the ROI level.

In-house software (BrainShow) was used to superimpose thresholded statistical maps over the individual brain.

SEP/fMRI co-registration

Correspondences between SEP components, fMRI data and underlying anatomical areas (in the inflated surface) were assessed using Talairach and Tournoux's (1988) stereotaxic coordinate system. MNI coordinates (Mazziotta et al., 1995) of the activation COGs were calculated through an automatic non-linear stereotaxic normalization procedure (Friston et al., 1995), performed using SPM99.

Behavioral experiment

Patient DM was tested four times: before the surgery (pre-test); 3 months after surgery during the PE (with the fixation cage still on); 6 months after surgery, 15 days after the removal of the Ilizarov fixation (post-test); and 6 months after the post-test (follow-up). To check the effect of natural growth, 7 age-matched

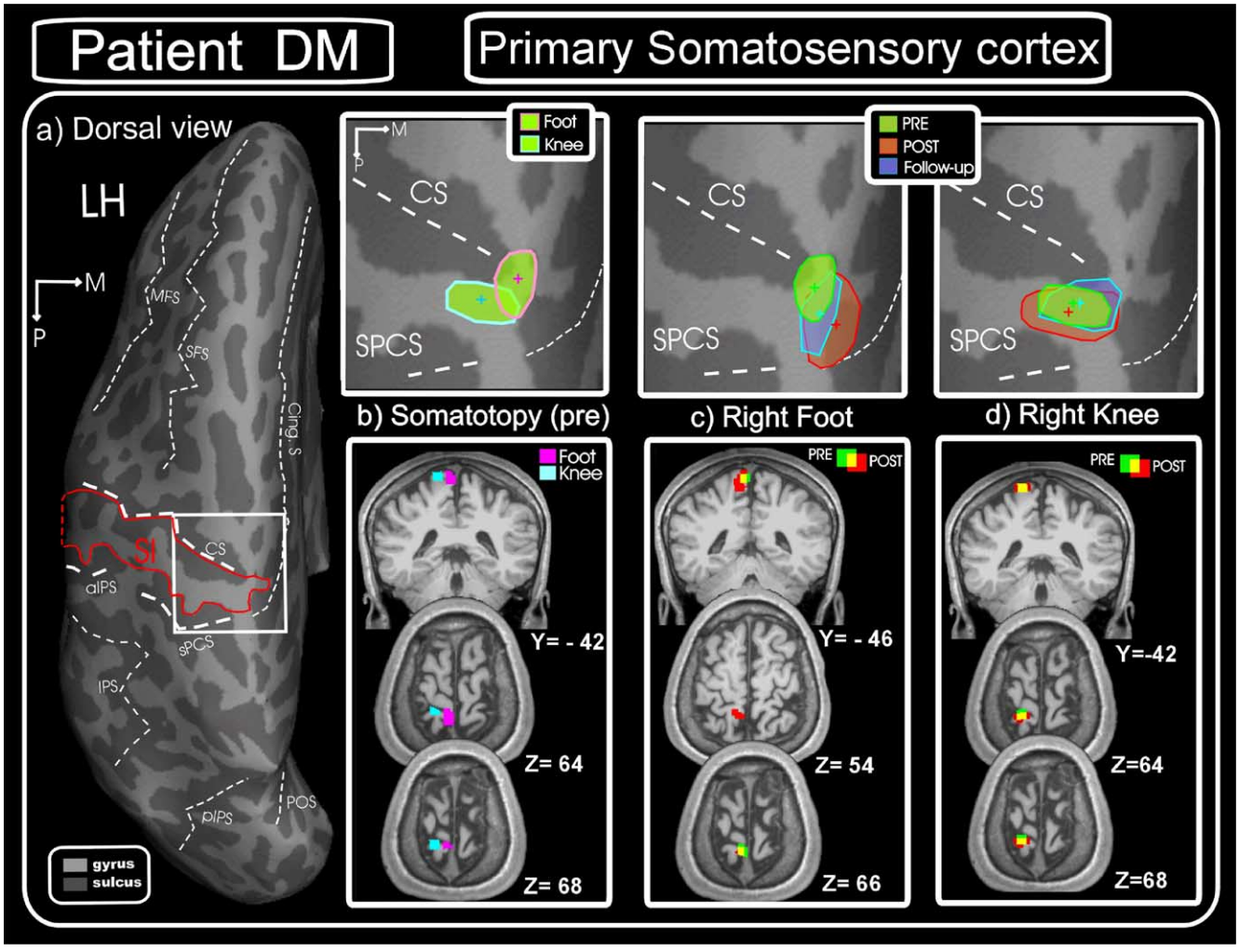

Fig. 3. fMRI data of patient DM in the pre-surgery, post-surgery and follow-up sessions. (a) Contralateral SI is indicated by a red outline and label on the inflated cortical surface reconstruction of the left hemisphere shown in dorsal view. Logos indicate two main orthogonal directions (anterior–posterior and medial–lateral). The main anatomical sulci (dark grey) have text labels: central sulcus (CS); superior post-central sulcus (sPCS); ascending intraparietal sulcus (aIPS); intraparietal sulcus (IPS); posterior IPS (pIPS); cingulate sulcus (CingS); parieto-occipital sulcus (POS); middle frontal sulcus (MFS); superior frontal sulcus (SFS). On the inflated surface, the fundus of both the central sulcus and the superior post-central sulcus, considered the anatomical landmark of SI, are indicated by a thick dashed white line. The white box indicates the cortical region considered in the three close-ups on the right. The first close-up (b) shows the somatotopic map of foot and knee we found in patient DM before surgery. The second (c) and third (d) close-ups show the foot and knee activation in SI, respectively, during the three sessions. As for the SEP experiment, green refers to the pre-test, red to the post-test and blue to the follow-up. The COG of each session is indicated with a colour-coded symbol (+) located in the centre of the outline. Significant fMRI activations for foot and knee stimulation are also displayed on three selected coronal and axial slices below each close-up (y and z coordinates are in native space).

controls (3 males, mean age 14.0 years ±1.02) were tested twice with an interval of 6 months between the first and the second evaluation. In the body schema test (Daurat-Hmeljiak et al., 1978), patient DM and the controls were asked to put one tile depicting a body part in the appropriate position (nine tiles: right/left leg–arm–hand–hemithorax and the neck; see Fig. 5) on an empty board where just face's contour was drawn. Subject performed the task on a desk seated in front of the examiner, no time limit was given. A score of 1 has been assigned for each tile correctly placed, according to a correction grid reproducing the whole body.

Results

Patient DM

SEP experiment

The spatio-temporal structure of the SEPs to stimulation of the right and left lower limbs in the three testing sessions is shown in Fig. 2. Since waveforms from the two limbs were very similar, results were averaged. *Pre-test:* Before the surgery, for foot stimulation, the earliest cortical component (P40) had an average onset latency of about 33 ms, a peak latency of 38 ms and peak amplitude of 1.5 μV. For knee stimulation, the earliest cortical component (P35) had an average onset latency of about 28 ms, a peak latency of 35 ms and peak amplitude of 0.8 μV (Fig. 2a green waveforms). As show in Fig. 2b, for both limbs, the foot P40 had a nearly radial distribution with a positive polarity at midline centro-parietal sites. The knee P35 had a tangential distribution with a positive polarity at contralateral parietal sites and a negative polarity at contralateral frontal sites (not shown in figure for the left knee). Fig. 2c shows the source localization of the SEP components on the actual patient's brain indicating that the P40 (Fig. 2c left) and the P35 (Fig. 2c right) were modeled by a single dipole located in contralateral centro-parietal areas close to the midline within the primary somatosensory cortex (SI). The residual variance for the P40 models was 1.91% for right stimuli (fMRI seeded model, see Materials and methods) and 1.50% for the left stimuli (unseeded model). The residual variance for the P35 models was 1.48% for right stimuli (fMRI seeded model) and 1.23% for the left stimuli (unseeded model). The two modeling strategies gave similar results also in terms of localization (compare left and right legs in Fig. 2c). The P35 source localization was more lateral than the P40 according to the somatotopic organization of SI (Penfield, 1950). *Post-test:* Two weeks after the fixation removal, for foot stimulation, the P40 was consistently delayed and reduced with an average onset latency of about 38 ms, a peak latency of 43 ms and peak amplitude of about 0.75 μV (Fig. 2a red waveform). For knee stimulation, the P35 did not change in terms of latency, amplitude or topography. The modification of the P40 was also visible in the scalp topography (Fig. 2b) and became more anterior after surgery. Dipole modeling (Fig. 2c) of P40 confirmed the source shift, becoming more anterior in orientation and more posterior and ventral in location (residual variance = 1.85% on the right and 1.53% on the left). *Follow-up:* Six months after the post-test, for foot stimulation, the P40 returned almost as it was before surgery with an average onset latency of about 34 ms, a peak latency of 40 ms and a peak amplitude of about 1.2 μV (Fig. 2a blue waveforms). Again, for knee stimulation the P35 did not change in terms of latency, amplitude topography or source localization. The re-normalization of the P40 is clearly visible in the scalp topography (Fig. 2b). As shown in Fig. 2c, the P40 dipole location and orientation are almost identical to the pre-test condition with an average residual variance of 1.63%. Overall,

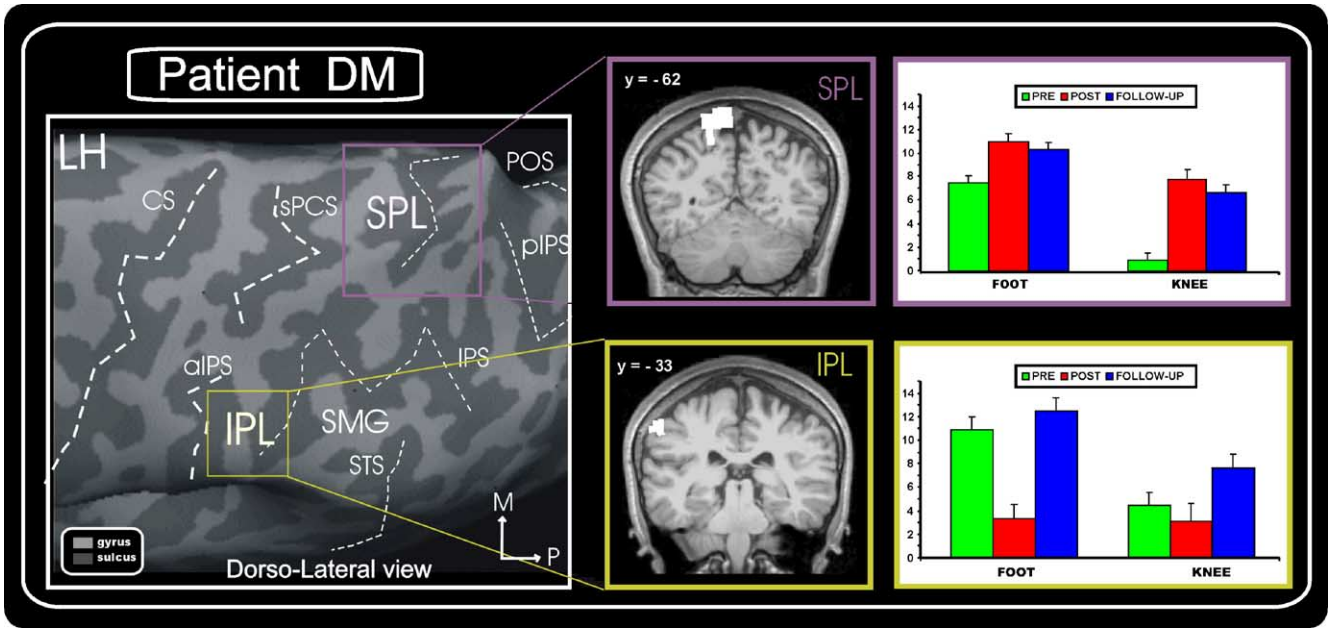

Fig. 4. fMRI data of patient DM in the pre-surgery, post-surgery and follow-up sessions outside contralateral SI. Colored boxes on the left inflated surface (shown in dorsolateral view) indicate the location of two functional ROIs (see Materials and methods for more details): contralateral superior parietal lobule (SPL) and inferior parietal lobule (IPL) (ipsilateral SPL not shown). The position of ROIs is also shown on two coronal slices in native coordinates. The histogram plots on the right show the estimated amplitude of the fMRI response (in arbitrary units) in the contralateral SPL (the ipsilateral one having a similar trend) and IPL for the foot and knee during each session. Error bars represent standard errors of parameter estimates. The main anatomical sulci (dark grey) and gyri have text labels: superior temporal sulcus (STS), supramarginal gyrus (SMG). Other anatomical labels are the same as in Fig. 3.

unseeded dipoles in the left hemisphere (LH) resulted about 5 mm more dorsal and anterior than the fMRI seeded dipoles in the right hemisphere (RH).

fMRI experiment

We first focused our analysis on DM's foot and knee cortical representation in the contralateral SI. Fig. 3a shows a dorsal view of the inflated cortical surface reconstruction of patient DM's left hemisphere. The white box drawn over the surface indicates the cortical region considered in the three close-ups displayed on the upper part of the figure (Figs. 3b, c and d). Below each close-up, the corresponding significant fMRI activation is also displayed on three selected slices (one coronal and two axial).

The first close-up (Fig. 3b) shows the right foot and knee activation we were able to map in patient DM before surgery (pre-test). They were located in the dorsomedial surface with a clear somatotopy, with the knee representation located more laterally than the foot one, as depicted in the classical somatosensory *homunculus* (Penfield, 1950). To our knowledge, the somatosensory representation of the knee has never been reported in a human neuroimaging experiment. This is also the first study that shows its dorsomedial location and its topographical and somatotopic relation to the map of the foot.

The second and third close-ups (Figs. 3c and d) show the evolution over time of the somatotopic maps of the foot and knee, respectively. In each close-up, results from the pre-test (green patch), post-test (red patch) and follow-up (blue patch) are overlapped together to facilitate comparisons. The center of gravity (COG) of each session is indicated with a color-coded symbol (+).

After the lengthening phase, the foot representation was enlarged and shifted ventrally to occupy a new region of the medial cortical surface. The COG of the whole activation was displaced by 6 mm. Six months later (follow-up), the more ventral activity during foot stimulation was no longer evident, and the COG was now displaced by only 3 mm (less than one voxel) with respect to the pre-lengthening session, thus suggesting an on-going restoration process of the initial before-lengthening representation (see Fig. 3c). Contrary to what we observed for the foot, the cortical representation of the knee was not affected by the lengthening phase. Indeed, it was detected in a virtually identical location in all three testing sessions (see Fig. 3d), and the distance between the COGs calculated before and after surgery was only 2 mm.

We then inspected the activity pattern caudally to SI in the associative parietal cortex (Fig. 4). Before the lengthening phase (pre-test), tactile stimulation of both segments activated the contralateral superior parietal lobule (SPL), including medially the precuneus, and the contralateral inferior parietal lobule (IPL), including the inferior post-central sulcus or ascending intraparietal sulcus (aIPS) and the more rostral portion of the supramarginal gyrus (SMG). A smaller SPL activation was also detected in the ipsilateral right hemisphere. Both superior and inferior parietal activation was wider for the foot than the knee, with the latter sharing the more lateral portion of the activation with the former. Interestingly, this trend brings to mind the somatotopic maps observed in SI.

After the lengthening phase, the signal significantly increased for both foot and knee in the superior parietal regions ($P < 10^{-4}$) and was still significantly higher at follow-up ($P < 10^{-4}$) (see Fig. 4, top histogram plots). On the contrary, in the contralateral inferior

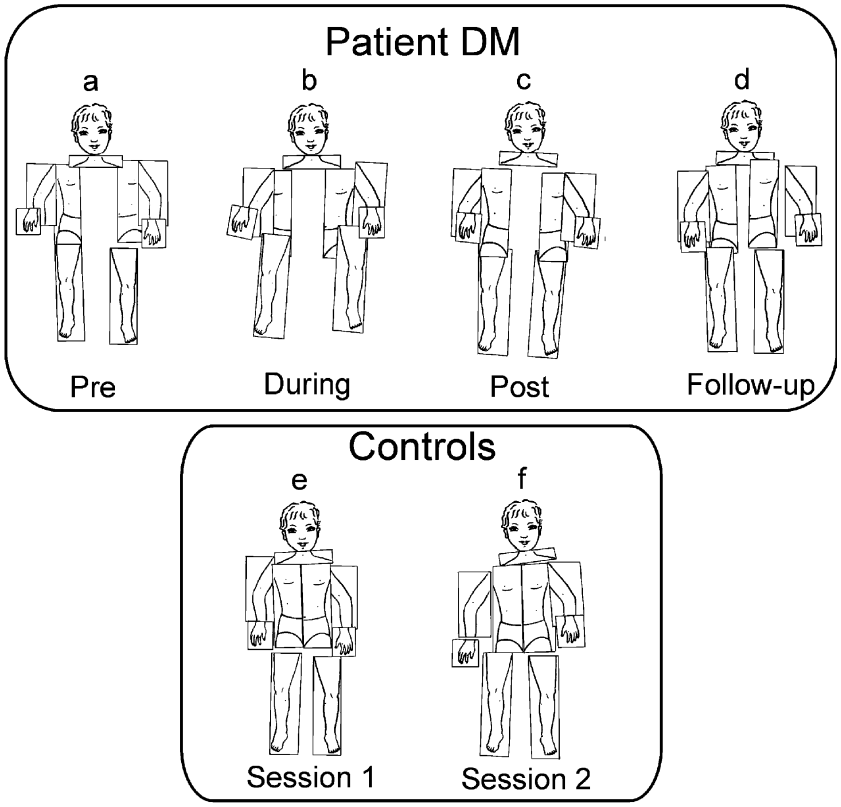

Fig. 5. Test of body schema: DM's dysmorphic performance in pre-test (a) and during immobilization (b). In the post-test (c) and follow-up (d), DM's performance was within normal range. Examples of one typical control subject's performance in the first (e) and second (f) assessment.

parietal region, we observed a signal decrease after the lengthening phase (foot: $P < 10^{-4}$; knee: $P = 0.2$), which reversed at follow-up (foot: $P < 10^{-4}$; knee: $P = 0.02$). See Fig. 4, lower histogram plots.

Behavioral experiment

In the pre-surgery assessment (pre-test), patient DM correctly placed seven out of nine tiles on the empty body contour, revealing a dysmorphic body representation corresponding to 7.6–8.5 years of age (Fig. 5a). During immobilization (3 months after surgery, with the fixation cage still on), performance was even more dysmorphic because 6/9 tiles were correctly placed, matching 6.6–7.5 years of age (Fig. 5b). In the post-test phase (6 months after surgery and 2 weeks after fixture removal), DM's performance (8/9 tiles) was within the normal range (Fig. 5c). As shown in Fig. 5d, an errorless performance (9/9 tiles) was obtained 6 months later (follow-up). In the post-test and follow-up phases, DM's body representation became completely comparable to that of control

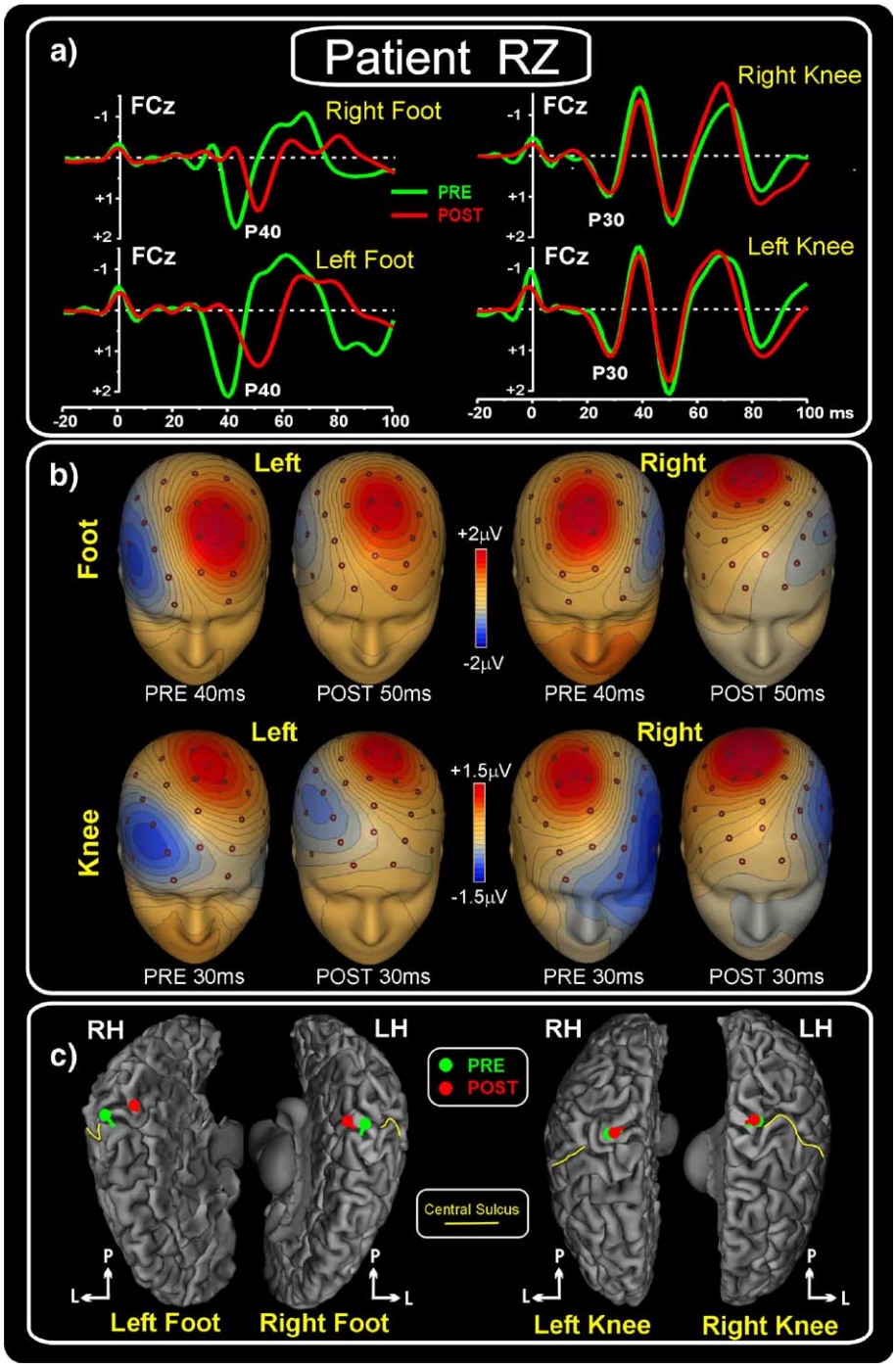

Fig. 6. SEP data of patient RZ in the pre-surgery and post-surgery session: (a) SEP waveforms showing the first P40 and P30 cortical component for foot and knee stimulation, respectively. (b) Scalp topography of P40 and P30 components. (c) Source model of studied components projected on the patient's anatomy. Logos indicate two main orthogonal directions (anterior–posterior and medial–lateral).

subjects, as shown in Figs. 5e and d (mean of correct tiles: first assessment = 8.33 ± 0.52, second assessment = 8.86 ± 0.38).

Patient RZ

The spatio-temporal structure of the SEPs to stimuli delivered in each lower limb location in patient RZ is shown in Fig. 6. Since waveforms from the two limbs were very similar, averaged results are given. *Pre-test:* Before surgery (Fig. 6a green waveforms), for foot stimulation, the earliest cortical component (P40) had an average onset latency of about 35 ms, a peak latency of 41 ms and a peak amplitude of 2.0 μV. For knee stimulation, the earliest cortical component (P30) had an average onset latency of about 22 ms, a peak latency of 29 ms and a peak amplitude of 1.30 μV. As shown in Fig. 6b, for both limbs, foot P40 had a tangential distribution with a positive polarity at midline and ipsilateral

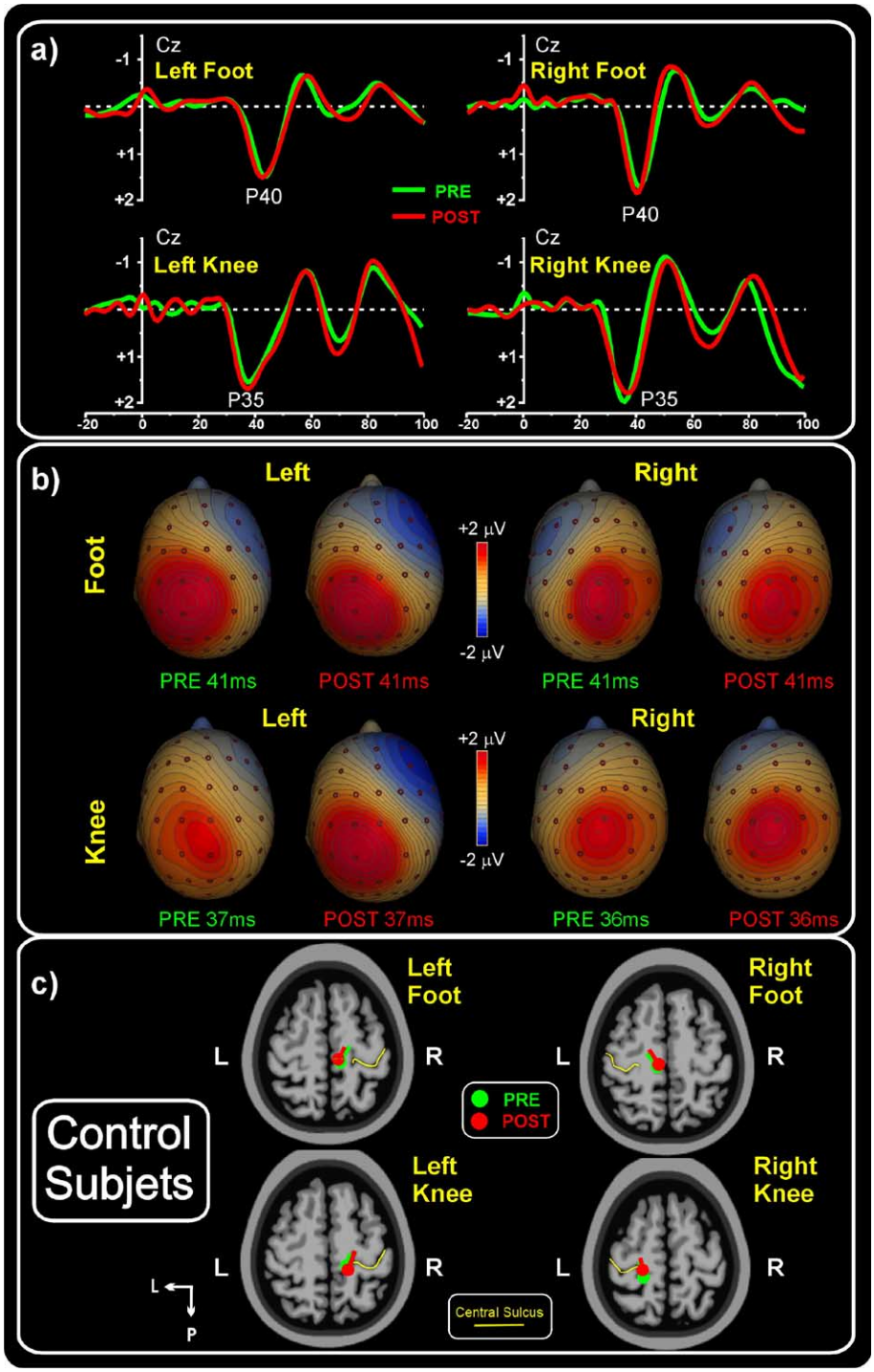

Fig. 7. SEP data of the control group in the two experimental sessions: (a) SEP waveforms showing the first P40 and P35 cortical component for foot and knee stimulation, respectively. (b) Scalp topography of P40 and P30 components. (c) Source model of studied components projected on the BESA template.

frontal sites and a negative polarity at contralateral frontal sites. Knee P30 had a tangential distribution with a positive polarity at ipsilateral central sites and a negative polarity at contralateral fronto-temporal sites. Fig. 6c shows the source localization of the SEP components on the patient's brain indicating that for both limbs the P40 and P30 were modeled by a single dipole located in contralateral centro-parietal areas close to the midline within SI. The averaged residual variance for the P40 and P30 models was 2.12% and 2.08%, respectively. *Post-test:* Two weeks after the fixation removal (Fig. 6a red waveforms), for foot stimulation, the P40 was consistently delayed and slightly reduced with an average onset latency of about 41 ms, a peak latency of 50 ms and peak amplitude of about 1.51 μV. For knee stimulation, the P30 did not change for latency, amplitude or topography. Modification of the P40 was also present in the scalp topography (Fig. 6b) and became more posterior after surgery. Dipole modeling (Fig. 6c) of P40 confirmed the source shift, becoming more posterior and ventral in location (average residual variance = 2.26%).

Control group

The average SEPs from the two age-matched control subjects is shown in Fig. 7. *Pre-test:* In the first recording session (Fig. 7a green waveforms), for foot stimulation, the P40 had an average onset latency of about 33 ms, a peak latency of 42 ms and peak amplitude of 1.75 μV. For knee stimulation, the P35 had an average onset latency of about 28 ms, a peak latency of 38 ms and peak amplitude of 1.80 μV. As show in Fig. 7b, foot P40 had a tangential distribution with a positive polarity at midline and ipsilateral parietal sites and a negative polarity at contralateral frontal sites. Knee P35 had a tangential distribution with a positive polarity at midline and ipsilateral centro-parietal sites and a negative polarity at contralateral frontal sites. As shown in Fig. 7c, P40 and P30 were modeled by a single dipole located in contralateral centro-parietal areas close to the midline within in SI. The residual variance was less than 1.82% for the P40 models and less than 1.93% for the P30 models. *Post-test:* Six months after the pre-test (Fig. 7a red waveforms), SEPs remained unchanged in terms of latency, amplitude, topography and source localization.

Discussion

To the best of our knowledge, present study is the first to investigate the somatosensory representation in achondroplastic patients submitted to PE of their lower limbs. Our results indicate that it is possible to document cortical, cognitive and peripheral plasticity following the PE by converging electrophysiological, neuroimaging and behavioral data.

Cortical reorganization

The main result concerns the functional reorganization of the primary somatosensory cortex (SI) due to leg extension. Converging SEP and fMRI data showed that for foot stimulation (below the surgical fracture), the progressive leg elongation induces modifications in term of delay, expansion and shifting of the afferent volley of sensory information to SI. These modifications are reduced 6 months after the elongation ends. No relevant changes were found to knee stimulation (above the surgical fracture) even if we cannot exclude that this negative result was due to a failure in detecting very small shifts (i.e., Ugurbil et al., 2003).

Comparing the *unseeded* dipole coordinates with those of the fMRI activations in response to the same stimuli, it appears that the two techniques yield convergent results. The single dipoles accounting for the P40 (foot) and P35 (knee) components, which represent the initial afferent volley of somatosensory information in area 3b of SI (e.g., Valeriani et al., 2000), were in close proximity to the SI activations obtained in the fMRI experiment, centered in the most anterior portion of the post-central gyrus. A consistent correspondence between the dipole shift and the fMRI COGs in all three testing sessions was also found, confirming the initial (post-surgical) ventral and posterior shift in activity and return to the original (pre-surgical) position 6 months later. Furthermore, when the P40 and P35 dipoles were *seeded* on the fMRI COGs and the orientations in the intervals used for the unseeded model were fitted, the residual variance remained low (less than 2.2%), thus increasing the spatial reliability of dipole modeling.

The post-test expansion may be due to the fact that for a certain period of time there are new computational needs. It is unlikely that these changes are connected with unmasking pre-existing lateral connections that might subserve fast learning (Karni et al., 1995). Rather, long-term experience-dependent reorganization suggests an improvement in synaptic connections between unit processing and modified sensory input from the enlarged body segments. It is worth noting that, in agreement with the present data, long-term reorganization can be changed back to a pre-existing organization even years after the pathological onset (Birbaumer et al., 1997).

Regarding the directionality of the shift on the medial surface inside SI, which was ventral and posterior, we might speculate that the enlarged body segments 'occupy' more space in the cortex between the foot and the knee, thus 'pushing' the foot representation in the 'expected' medial direction. The posterior component of the shift, instead, suggests that at the end of the surgical lengthening, there was greater involvement of the more caudal subarea of SI (area 2), which receives inputs mainly from the deep receptors of the joints (Kaas, 1993) and whose neurons respond to more complex cutaneous stimuli or to active tactile discrimination tasks (Bodegard et al., 2001).

The greater involvement of higher level regions of somatosensory processing following the progressive elongation of the limbs is supported by the further activation observed outside SI. In fact, a second relevant finding of the present work regards the post-test expansion observed caudally to SI in the associative parietal cortex of the superior parietal lobules of both hemispheres. Early experiments in monkey showed that SPL is related to the somatosensory system and that main afferent inputs come from SI (Sakata et al., 1973; Mountcastle et al., 1975). In particular, SPL is crucially involved in visuomotor coordination coding the spatial relationships between body parts and between the body and the surrounding environment (e.g., Graziano, 2001). After the change in the length of the lower limbs, these functions must have become heavily involved in providing the patient a correct control of his movements and interactions with the world. It is reasonable to think that such elaboration continued well after the post-test session (2 weeks after the end of the elongation), for the entire period during which DM re-acquired skilled behavior with his new physical dimensions. It is very important to recall here (also for its possible clinical implications) that at the last observation DM still reported difficulty with some movements requiring the right proportions between body segments, such as the ability to stand

up from the floor without help. This was probably due to the fact that at the time his PE regarded only the shinbone since he was waiting to start PE of the thigh bone and was therefore in a condition of lever imbalance. After all these considerations, it is not surprising that the reorganization observed in the SPL was qualitatively different from that observed in SI. In fact, it appeared to be more sustained in time, with a stronger and larger activation still evident at follow-up. Furthermore, it was not restricted to the foot but regarded also the knee, in agreement with a more integrated sensorimotor role of the involved regions.

Another interesting finding of the present work is the constant activation, across sessions and conditions, of an inferior parietal region located in the ascending IPS and anterior supramarginal gyrus. Human SMG corresponds to monkey area PF (or 7b), in the IPL, which contains many neurons responding to passive somatosensory stimulation (Hyvärinen, 1981; Gallese et al., 2002). This activation may also correspond to the so-called IP1 and IP2 regions in the rostral part of the IPS and immediately caudal to it (Choi et al., 2002), both found to be activated in a recent study by the somatosensory stimulation of the foot and susceptible to task-related attentional modulation (Young et al., 2004). Alternatively, the inferior parietal activation observed here might represent the contralateral secondary somatosensory area (SII), even though it is slightly displaced respect to that described in normal subjects (e.g., Del Gratta et al., 2000; Del Gratta et al., 2002; Ferretti et al., 2003). This interpretation is not implausible given that an activation of area SII is often found with simple non-painful tactile stimulation and not just in the canonical position but also quite anterior to it, recently called *anterior SII* (e.g., Ferretti et al., 2004). It is also possible that the non-canonical position of SII is due to the neuroanatomic abnormalities present in the achondroplastic brains. To our knowledge, the location of area SII in this kind of patients has never been mapped before; thus, there are no other reference points. Contrary to SPL, this inferior parietal region showed a significant signal decrease after the PE, which went back to the original values at follow-up, thus paralleling the evolution of the signal in SI but with opposite sign. It is reasonable to consider the observed pattern in the light of a plastic process of reorganization which, together with more active regions after the PE, includes also regions showing less activity.

Moreover, given the fMRI results described so far (specifically, the different evolution over time of the functional changes in and outside SI for the two body segments, and even more importantly, the difference between IPL and SPL in terms of signal increase/decrease), we can exclude a trivial specific effect of a generally higher signal in the post-test respect to the pre-test session.

Cognitive reorganization

Behavioral data show that before surgery DM had a dysmorphic perception of his body. He appeared to be somewhat aware of his atypical growth as showed in Fig. 5. A pathological modification was also present when he was tested 3 months later. At that time, probably due to the knowledge and expectation of the occurring changes in size, his body representation became fragmented with frequents overlapping of body parts (Fig. 5b). Furthermore, the presence of the Ilizarov fixation could have influenced the performance. However, in the following assessments (soon after prosthesis removal and 6 months later), DM performed as normal age-matched controls. These results clearly demonstrate that cognitive re-organization of body schema strictly paralleled the physical changes that DM underwent to reach a proportionate structure.

There are several reasons why a direct comparison cannot be easily made between the observed neurophysiological changes and the patient's performance on the body schema test. First, we recorded SEPs and fMRI signal only during a simple passive tactile task and not during higher level cognitive tasks. Second, while the pre-surgery cortical organization appeared to be normal, the pre-surgery body schema of patient DM was dysmorphic. It is not surprising that, with different starting points, the two measures had a different evolution over time.

Peripheral reorganization

SEP latency of the first cortical components (N35 and N40) studied here is clear markers of sensory peripheral reorganization due to the PE. It is known that the N35 and the N40 latencies are positively correlated with the distance from the stimulation site to SI (Bartel et al., 1987; Mutoh et al., 1989). In present study, we found a latency increase N40 of up to 10 ms in the post-surgery test and a rebound in the follow-up study suggesting a temporary demyelination of sensory fibers (no neurographic data regarding temporary demyelination due to nerve extension are present in literature). No modification of the N35 confirms and limits the peripheral adjustment at the level of the leg.

Results should be cautioned because there is no evidence that the plastic changes found in present study are exclusively due to the leg extension but may also reflect the external fixation device which was worn for 6 months.

Conclusions

Taken together, the present results suggest that the human cerebral cortex overcomes major modification of peripheral sensory representation with remarkable adaptation. Passing through a period of more or less sustained disorganization, the cerebral cortex appears capable of "computational plasticity" allowing dynamic reorganization of body representation.

Acknowledgments

This work is supported by "Fondazione Santa Lucia" grant and MURST grants.

References

Bartel, P., Conradie, J., Robinson, E., Prinsloo, J., Becker, P., 1987. The relationship between median nerve somatosensory evoked potential latencies and age and growth parameters in young children. Electroencephalogr. Clin. Neurophysiol. 68, 180–186.

Birbaumer, N., et al., 1997. Effect of regional anaesthesia on phantom limb pain are mirrored in changes in cortical reorganization. J. Neurosci. 17, 5503–5508.

Birch, J.G., Samchukov, M.L., 2004. Use of the Ilizarov method to correct lower limb deformities in children and adolescents. J. Am. Acad. Orthop. Surg. 12, 144–154.

Bodegard, A., Geyer, S., Grefkes, C., Zilles, K., Roland, P.E., 2001. Hierarchical processing of tactile shape in the human brain. Neuron 31, 317–328.

Buonomano, D.V., Merzenich, M.M., 1998. Cortical plasticity: from synapses to maps. Annu. Rev. Neurosci. 21, 149–186.
Cattaneo, R., Villa, A., Catagni, M., Tentori, L., 1988a. Limb lengthening in achondroplasia by Ilizarov's method. Int. Orthop. 12, 173–179.
Cattaneo, R., Villa, A., Catagni, M., Tentori, L., 1988b. Strategies for limb lengthening in achondroplasia using the Ilizarov method: the experience of the hospital of Lecco, Italy. Basic Life Sci. 48, 381–388.
Choi, H.J., 2002. Cytoarchitectonic mapping of the anterior ventral bank of the intraparietal sulcus in humans. NeuroImage 16, 200–238.
Dale, A.M., Fischl, B., Sereno, M.I., 1999. Cortical surface-based analysis: I. Segmentation and surface reconstruction. NeuroImage 9, 179–194.
Daurat-Hmeljiak, C., Stambak, M., Berges, J., 1978. Il test dello schema corporeo. Una prova di conoscenza e costruzione dell'immagine del corpo. Organizzazioni Speciali, Firenze.
Del Gratta, C., et al., 2000. Topographic organization of the human primary and secondary somatosensory areas: an fMRI study. NeuroReport 11, 2035–2043.
Del Gratta, C., et al., 2002. Topographic organization of the human primary and secondary somatosensory cortices: comparison of fMRI and MEG findings. NeuroImage 17, 1373–1383.
Dettmers, C., et al., 1999. Abnormal motor cortex organization contralateral to early upper limb amputation in humans. Neurosci. Lett. 263, 41–44.
Dettmers, C., et al., 2001. Increased excitability in the primary motor cortex and supplementary motor area in patients with phantom limb pain after upper limb amputation. Neurosci. Lett. 307, 109–112.
Diamond, M.E., Peterson, R.S., Harris, J.A., Panzeri, S., 2003. Investigation into the organization of information in sensory cortex. J. Phys. (Paris) 97, 529–536.
Di Mario Jr., F.J., Ramsby, G.R., Burleson, J.A., Greensheilds, I.R., 1995. Brain morphometric analysis in achondroplasia. Neurology 45, 519–524.
Di Russo, F., Martínez, A., Sereno, M.I., Pitzalis, S., Hillyard, S.A., 2002. The cortical sources of the early components of the visual evoked potential. Hum. Brain Mapp. 15, 95–111.
Di Russo, F., et al., 2005. Identification of the neural sources of the pattern-reversal VEP. NeuroImage 24, 874–886.
Duvernoy, H., 1991. The human brain. Surface, Tri-dimensional sectional anatomy and MRI. Springer-Verlag, Wien-New York.
Farné, A., Roy, A.C., Giraux, P., Dubernard, J.M., Sirigu, A., 2003. Face or hand, not both: perceptual correlates of reafferentation in a former amputee. Curr. Biol. 12, 1342–1346.
Ferretti, A., et al., 2003. Functional topography of the secondary somatosensory cortex for nonpainful and painful stimuli: an fMRI study. NeuroImage 20, 1625–1638.
Ferretti, A., et al., 2004. Functional topography of the secondary somatosensory cortex for nonpainful and painful stimulation of median and tibial nerve: an fMRI study. NeuroImage 23, 1217–1225.
Fischl, B., Sereno, M.I., Dale, A.M., 1999. Cortical surface-based analysis: II. Inflation, flattening, and a surface-based coordinate system. NeuroImage 9, 195–207.
Flor, H., et al., 1995. Phantom limb pain as perceptual correlate of cortical reorganization following arm amputation. Nature 375, 482–484.
Friston, K.J., et al., 1995. Spatial registration and normalization of images. Hum. Brain Mapp. 2, 165–189.
Gallese, V., Fadiga, L., Fogassi, L., Rizzolatti, G., 2002. In: Prinz, W., Hommel, B. (Eds.), In Common Mechanisms In Perception and Action: Attention and Performance. Oxford Univ. Press, UK, pp. 334–355.
Giraux, P., Sirigu, A., Schneider, F., Dubernar, J.M., 2001. Cortical reorganization in motor cortex after graft of both hands. Nat. Neurosci. 4, 691–692.
Graziano, M.S., 2001. Is reaching eye-centered, body-centered, hand-centered or a combination? Rev. Neurosci. 12, 175–185.
Hyvärinen, J., 1981. Regional distribution of functions in parietal association area 7 of the monkey. Brain Res. 206, 287–303.
Ilizarov, G.A., Deviatov, A.A., 1971. Surgical elongation of the leg. Ortop. Travmatol. Protez. 32, 20–25.
Kaas, J.H., 1993. The functional organization of somatosensory cortex in primates. Anat. Anz. 175, 509–518.
Karni, A., et al., 1995. Functional MRI evidence for adult motor cortex plasticity during motor skill learning. Nature 377, 155–158.
Knecht, S., et al., 1991. Plasticity of plasticity? Changes in the pattern of perceptual correlates of reorganization after amputation. Brain 121, 717–724.
Mazziotta, J.C., Toga, A.W., Evans, A., Fox, P., Lancaster, J., 1995. A probabilistic atlas of the human brain: theory and rationale for its development. The International Consortium for Brain Mapping (ICBM). NeuroImage 2, 89–101.
Mountcastle, V.B., Lynch, J.C., Georgopoulus, A., Sakata, H., Acuna, C., 1975. Posterior parietal association cortex of the monkey: command functions for operations within extrapersonal space. J. Neurophisiol. 38, 871–908.
Mueller, S.M., 1980. Enlarged cerebral ventricular system in infant achondroplastic dwarf. Neurology 30, 767–769.
Mutoh, K., Hojo, H., Mikawa, H., 1989. Maturational study of short-latency somatosensory evoked potentials after posterior tibial nerve stimulation in infants and children. Electroencephalogr. Clin. Electroencephalogr. 20, 91–102.
Penfield, W., 1950. The Cerebral Cortex of The Man. MacMillan, New York.
Ramachandran, V.S., Rogers-Ramachandran, D., Stewart, M., 1992. Perceptual correlates of massive cortical reorganization. Science 258, 1159–1160.
Rorden, C., Brett, M., 2000. Stereotaxic display of brain lesions. Behav. Neurol. 12, 191–200.
Sakata, H., Takaoka, Y., Kawarasaki, A., Shibutani, H., 1973. Somatosensory properties of neurons in the superior parietal cortex (area 5) of the rhesus monkey. Brain Res. 64, 85–102.
Talairach, J., Tournoux, P., 1988. Co-Planar Stereotaxic Atlas of the Human Brain. Thieme, New York.
Thompson, N.M., et al., 1999. Neuroanatomic and neuropsychological outcome in school-age children with achondroplasia. Am. J. Med. Genet. 88, 145–153.
Ugurbil, K., et al., 2003. Ultrahigh field magnetic resonance imaging and spectroscopy. Magn. Reson. Imaging 21, 1263–1281.
Valeriani, M., Restuccia, D., La Pera, D., Barba, C., Tonali, P., 2000. Scalp distribution of the earliest cortical somatosensory evoked potential to tibial nerve stimulation: proposal of a new recording montage. Clin. Neurophysiol. 111, 1469–1477.
Wall, J.T., Wang, J.X., 2002. Human brain plasticity: an emerging view of the multiple substrates and mechanisms that cause cortical changes and related sensory dysfunctions after injuries of sensory inputs from the body. Brain Res. Rev. 39, 181–215.
Young, J.P., et al., 2004. Somatotopy and attentional modulation of the human parietal and opercular regions. J. Neurosci. 24, 5391–5399.